

# The effect of material matching on the stress-induced power degradation for light-redirecting-ribbon-based silicon photovoltaic modules

X F Gou<sup>1,2</sup>, H Zhuang<sup>2,3</sup>, J Zhu<sup>2</sup> and X Y Li<sup>1</sup>

<sup>1</sup>Beijing University of Technology, 100124, Beijing, China

<sup>2</sup>CECEP Solar Energy Technology (Zhenjiang) Co. Ltd, 212132, Zhenjiang, China

<sup>3</sup>E-mail: zhuanghao@cecsec.cn

**Abstract.** Light redirecting ribbons (LRR) have recently been adopted in crystalline silicon modules in PV industry. The introduction of this LRR may bring additional stress at the boundary of the busbar/wafer contact, which may probably lead to higher power loss after aging. The thermal cycle and electroluminescence (EL) test are employed in this work to investigate this stress-induced power degradation for LRR-based crystalline silicon modules. The obtained results demonstrate that with increase in the thickness of the EVA encapsulant or the decrease in the thickness of the LRR, the power degradation induced by stress can be effectively diminished.

## 1. Introduction

Reliability and degradation of photovoltaic (PV) modules are an important concern to ensure the lifetime of PV modules longer than 25 years. PV module may degrade due to different environmental factors, such as irradiation, temperature, humidity and mechanical shock [1-4]. Several types of module degradation [5-11] can be triggered by each one of these various factors that induce corrosion, discoloration, delamination, cell breakage and cracking.

Stimulated by the strong demand for high-efficiency module products, light redirecting ribbons (LRR) have recently been adopted in high performance crystalline silicon PV modules to increase the power output. The light redirecting ribbon has delicately designed microstructures, which can reflect the incident light with an optimized angle to increase the chance of being reutilized by the cells. However, the introduction of this extra redirecting ribbon, which is usually over one hundred microns, can increase the risk of stress induced degradation of PV modules.

In this paper, thermal cycle test and electroluminescence measurement are adopted to investigate the stress induced power degradation of LRR-based modules. The influence of different thicknesses of the encapsulant and redirecting ribbon on the degradation level was systematically studied. The maximum output power and the electroluminescence were all measured after 200 thermal cycle test for each module. The electroluminescence images are in accordance with the level of module power loss. The obtained results demonstrate that with increase in the thickness of the EVA encapsulant or decrease in that of the LRR, the power degradation induced by stress can be effectively reduced. Our results can provide a guide for the thickness selection of encapsulant and LRR for LRR-based modules.



## 2. Experimental

Different module specimens were produced according to the industrial process at CECEP solar (Zhenjiang) with a standard composition of glass/EVA/cell/EVA/backsheet. Light redirecting ribbons of different thicknesses were assembled on the surface of the conventional interconnecting ribbon under heating using Autowell stringer. Thermal cycle test was performed according to the IEC 61215 standard (TC 200 cycles between  $-40^{\circ}\text{C}$  and  $+85^{\circ}\text{C}$  with a dwell time of 30 minutes at the temperature extremes). The power output and EL measurements were performed for each module after TC200 test. The maximum power output was measured under STC ( $25^{\circ}\text{C}$ ,  $1000\text{ W/m}^2$ , AM 1.5).

## 3. Results and Discussion

### 3.1. Mechanism of stress

With the assistance of the bottom hot melt EVA, the light redirecting ribbon can be directly pasted to the welding ribbon under heating. For a conventional PV module, highly conductive ribbons (i.e., usually tin-coated copper ribbon) are soldered to the busbars from the front of one cell to the back of a neighbouring cell for current transport. It has already been noted that the coefficient of thermal expansion (CTE) is quite different between copper ( $17 \times 10^{-6}\text{ K}^{-1}$ ), silicon ( $3 \times 10^{-6}\text{ K}^{-1}$ ) and glass ( $9 \times 10^{-6}\text{ K}^{-1}$ ) [12]. Their difference in CTE will cause a buildup of internal stresses as the materials cool down from high temperature. During the module lifetime of outdoor use, it may repeatedly undergo the high-temperature low-temperature cycle. Thus, stress often accumulates at the boundary of the busbar/wafer contact (figure 1). Furthermore, the introduction of this LRR layer on the welding ribbon will definitely increase the risk of stress induced degradation if no parameter of the materials is changed.

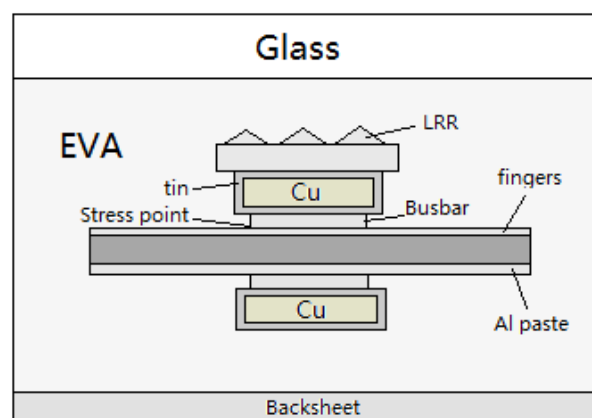


**Figure 1.** Scheme of the stress point of the LRR-based PV module.

### 3.2. EVA thickness effect on the power degradation

Currently, 0.45 mm thick EVA is widely adopted for PV module encapsulation. To investigate whether the introduction of LRR will cause much higher degradation when encapsulated with normal 0.45 mm thick EVA, LRR with different thicknesses, 0.115 mm and 0.15 mm, was employed for the LRR-based module specimen encapsulation. After encapsulation, the initial performance of the modules was measured. Then, the modules were put into the climate chambers to undergo the TC200 test. After the TC200 test, the typical EL images of the modules were measured and presented in figure 2. As can be seen, after the aging test, severe cell breakage and cracking problems occurred for both types of modules with different LRR thicknesses, suggesting that a much thicker EVA film should be used [13].

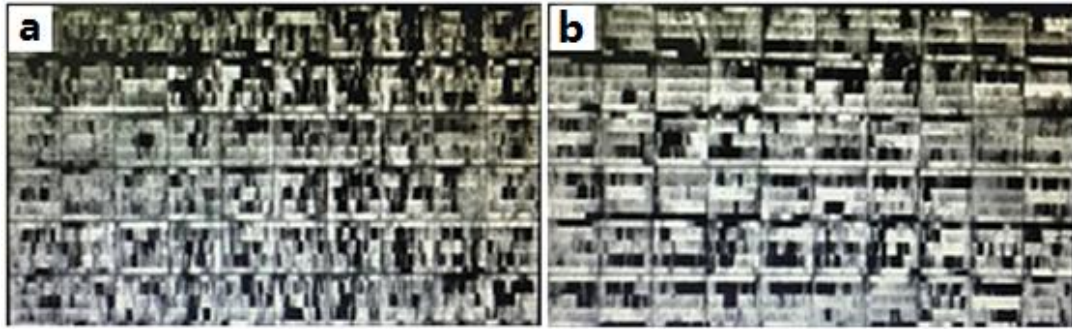


**Figure 2.** EL images of modules with 0.45 mm EVA after TC200 test: a) LRR 0.15 mm; b) LRR 0.115 mm.

Then the thickness of the front EVA film was increased to 0.65 mm, and modules were encapsulated with the same process. The LRR thickness in module A and B is 0.115 mm, and that in C and D is 0.15 mm. The electrical performance of the modules before and after the TC200 test was measured and listed in table 1. As can be seen, after the TC200 test, still high degradation level for the modules was observed. However, a LRR-thickness dependent degradation could be noted. The  $P_{max}$  of module A and B with thinner LRR degraded 5.96% and 4.85%, respectively. While the  $P_{max}$  of module C and D with thicker LRR degraded 6.21% and 5.17%, respectively.

**Table 1.** Performance degradation of modules with 0.65 mm EVA and different LRR thicknesses.

Module	LRR Thickness	Test Item	$P_{max}$	$V_m$	$I_m$	$V_{oc}$	$I_{sc}$	FF	CTM	$P_{max}$ Degradation
A	0.115mm	Initial	274.01	31.21	8.78	38.24	9.27	77.30 %	100.90 %	5.96%
		After TC200	257.69	29.64	8.69	38.10	9.26	73.06 %	94.89%	
B	0.115mm	Initial	274.18	31.16	8.80	38.17	9.29	77.30 %	100.97 %	4.85%
		After TC200	260.88	29.88	8.73	38.05	9.30	73.69 %	96.07%	
C	0.15mm	Initial	272.79	31.11	8.77	38.16	9.35	76.40 %	100.45 %	6.21%
		After TC200	255.86	29.52	8.67	37.98	9.30	72.39 %	94.22%	
D	0.15mm	Initial	272.99	31.09	8.78	38.18	9.27	77.10 %	100.53 %	5.17%
		After TC200	258.87	29.82	8.68	38.00	9.31	73.17 %	95.33%	

The  $V_{oc}$ ,  $I_{sc}$ ,  $FF$  and  $P_{max}$  of modules with 0.65 mm EVA before and after TC200 test are depicted in figure 3. It shows that the degradation in the maximum output power is mainly driven by the loss in  $FF$  and the losses in  $V_{oc}$  and  $I_{sc}$  are quite small. Changes in electrical parameters can be explained below using electro-luminescence results. Figure 4 shows the EL measurement performed on the modules after the TC test. Compared with those using 0.45 mm EVA, cracks and breakage in the cells have been much improved. However, still evident in-active regions and finger defects can be noted. In-active regions of the cell may arise from the detachment of a part of the cell from the busbar [8]. These results demonstrate that increase in the EVA film thickness can effectively decrease the stress induced degradation level and thinner LRR is more desirable for its lower degradation level.

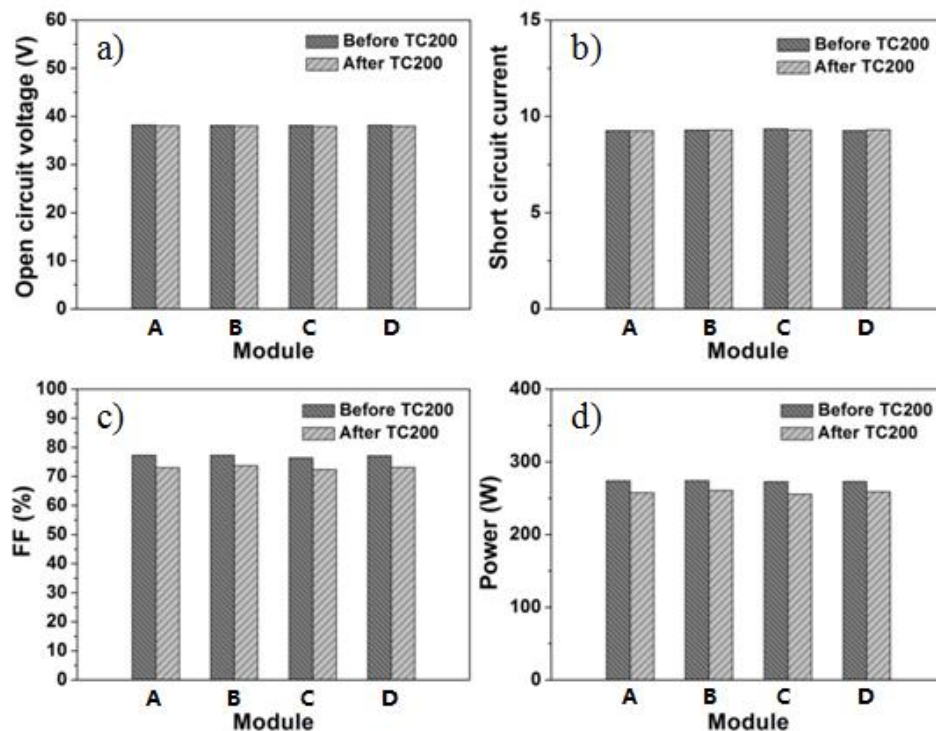


**Figure 3.** The  $V_{oc}$ ,  $I_{sc}$ ,  $FF$  and  $P_{max}$  of modules with 0.65 mm EVA before and after TC200 test.

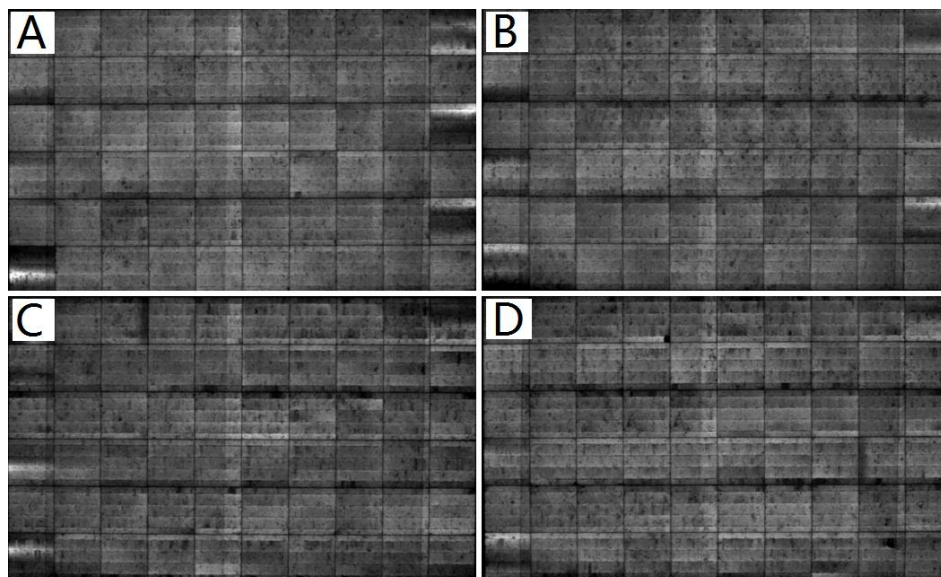


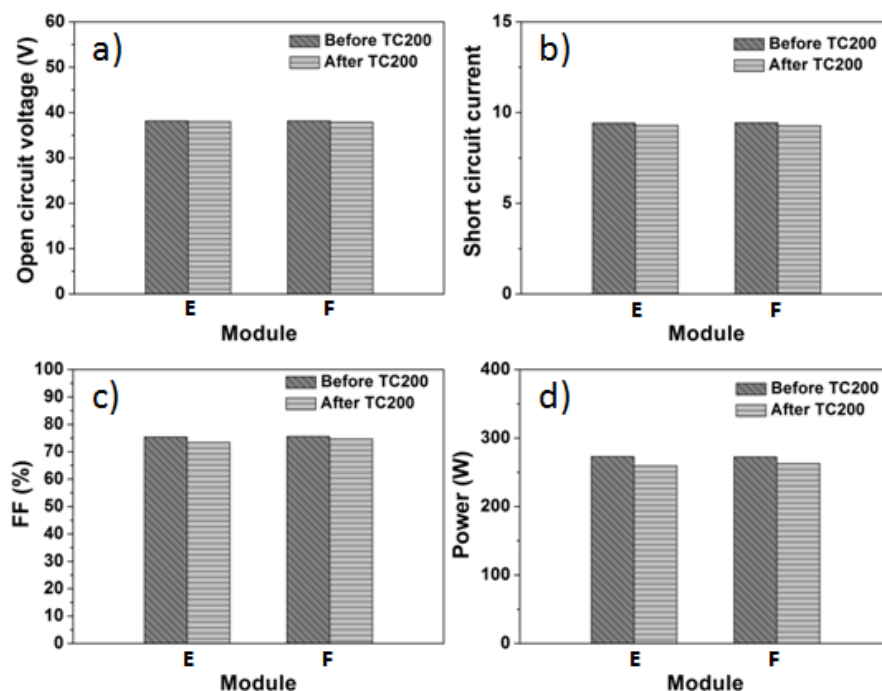
**Figure 4.** EL images of modules with 0.65 mm EVA after TC 200 test: A) and B) LRR 0.115 mm; C) and D) LRR 0.15 mm.

Since the power degradation level is still higher than the permitted maximum 5% degradation, an even thicker EVA was prepared and attempted. The electrical performance of the modules before and after the TC200 test was measured and summarized in table 2. The LRR thickness in module E is 0.15 mm, and that in F is 0.115 mm. After TC200 test, the  $P_{max}$  of module E with thicker LRR degraded 5.02% while the  $P_{max}$  of module F with thinner LRR degraded 3.52%, which is nearly 30% less than the module with 0.035 mm thicker LRR.

**Table 2.** Performance degradation of modules with 0.8 mm EVA and different LRR thicknesses.

Module	LRR Thickness	Test Item	$P_{max}$	$V_m$	$I_m$	$V_{oc}$	$I_{sc}$	FF	CTM	$P_{max}$ Degradation
E	0.15mm	Initial	273	30.6	8.87	38.2	9.42	75.40%	99.98%	5.02%
		After TC200	259.3	29.8	8.69	38	9.30	73.40%	94.96%	
F	0.115mm	Initial	272.6	30.6	8.90	38.2	9.44	75.60%	99.83%	3.52%
		After TC200	263	30.1	8.74	37.9	9.28	74.70%	96.31%	

The  $V_{oc}$ ,  $I_{sc}$ ,  $FF$  and  $P_{max}$  of modules with 0.8 mm EVA before and after TC200 test are depicted in figure 5. It shows that the degradation in the maximum output power is mainly driven by the loss in  $FF$  and  $I_{sc}$ . Changes in electrical parameters can be explained below using electro-luminescence results. Figure 6 shows the EL measurement performed on the modules after the TC test. Compared with those using 0.65 mm EVA, cracks and in-active regions in the cells have been largely improved. However, still evident in-active regions and finger defects can be noted for the 0.15 mm LRR-based module. In contrast, for the 0.115 mm LRR-based module, few in-active regions of the cell due to detachment of a part of the cell from the busbar can be obviously observed, indicating reduced stress inside the module at the boundary of the busbar/wafer contact. These results demonstrate that further increase in the EVA film thickness to 0.8 mm can decrease the degradation of 0.115 mm LRR-based module to a reasonable level that meets the IEC 61215 standard.

**Figure 5.** The  $V_{oc}$ ,  $I_{sc}$ ,  $FF$  and  $P_{max}$  of modules with 0.8 mm EVA before and after TC200 test.



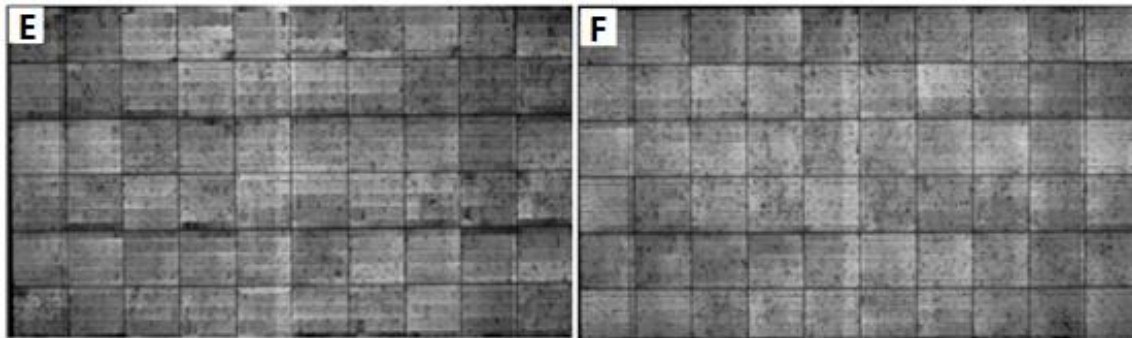


**Figure 6.** EL images of modules with 0.8 mm EVA after TC200 test: E) LRR 0.15 mm; F) LRR 0.115 mm.

### 3.3. Insulation performance

The insulation performance of the modules before and after TC200 test was also measured and summarized in table 3. The area of module samples is  $1.63 \text{ m}^2$ , which sets the pass criteria at  $24.4 \text{ M}\Omega$  [14]. As can be seen, after the TC200 test, no obvious degradation in the insulation performance is observed. The insulation resistance for module E and F are both higher than  $2000 \text{ M}\Omega$  before and after the TC200 aging test. All these obtained results suggest that 0.8 mm EVA is adequate to endure the stress induced degradation in 0.115 mm LRR-based modules.

**Table 3.** The insulation performance of the modules before and after TC200 test.

Module	State	Sample Area ( $\text{m}^2$ )	Standard ( $\text{M}\Omega$ )	Experimental Value ( $\text{M}\Omega$ )
E	Initial	1.63	>24.4	>2000
	After TC200			>2000
F	Initial	1.63	>24.4	>2000
	After TC200			>2000

## 4. Conclusion

The experimental results indicate that additional stress does exist in the module because of the introduction of light redirecting ribbon (LRR). The thermal cycle aging results demonstrate that with increase in the thickness of the EVA encapsulant or the decrease in the thickness of the LRR, the power degradation induced by stress can be effectively decreased. The EL images of the modules before and after the TC200 test are in correspondence with power degradation extent. The LRR-based modules showed good insulation performance both before and after the TC200 test. Our results provide a guide for the thickness selection of encapsulant and LRR for LRR-based modules.

## Acknowledgements

This study was financially supported by the research program 17RD2 CECEP (Zhenjiang).

## List of symbols and abbreviations

EVA: ethylene vinyl acetate copolymer

$P_{\text{max}}$ : maximum power output

$V_{\text{m}}$ : voltage at maximum power point

$I_{\text{m}}$ : current at maximum power point

$V_{\text{oc}}$ : open circuit voltage

$I_{\text{sc}}$ : short circuit current

FF: fill factor

CTM: cell to module gain

## References

- [1] Quintana M A, King D L, McMahon T J and Osterwald C R 2002 Commonly observed degradation in field-aged photovoltaic modules *In: Proc. 29th IEEE Photovoltaic Specialists Conference* 1436-39
- [2] Osterwald C R and McMahon T J 2009 History of accelerated and qualification testing of terrestrial photovoltaic modules: a literature review *Prog. Photovolt.: Res. Appl.* **17** 11-33
- [3] Munoz M A, Alonso-Garcia M C, Nieves V and Chenlo F 2011 Early degradation of silicon PV modules and guaranty conditions *Sol. Energy* **85** 2264-74
- [4] Vazquez M and Ignacio R S 2008 Photovoltaic module reliability model based on field degradation studies *Prog. Photovolt.: Res. Appl.* **16** 419-33
- [5] Hoffmann S and Koehl M 2014 Effect of humidity and temperature on the potential-induced degradation *Prog. Photovolt.: Res. Appl.* **22** 173-79
- [6] Duerr I, Bierbauma J, Metzgera J, Richtera J and Philippa D 2016 Silver grid finger corrosion on snail track affected PV modules-investigation on degradation products and mechanisms *Energy Procedia* **98** 74-85
- [7] Zarmai M T, Ekere N N, Oduoza C F and Amalu E H 2017 Evaluation of thermo-mechanical damage and fatigue life of solar cell solder interconnections *Robot. Comput.-Integr. Manuf.* **47** 37-43
- [8] Khatri R, Agarwal S, Saha I, Singh S K and Kumar B 2011 Study on long term reliability of photo-voltaic modules and analysis of power degradation using accelerated aging tests and electroluminescence technique *Energy Procedia* **8** 396-401
- [9] Kempe M D, Dameron A A and Reese M O 2014 Evaluation of moisture ingress from the perimeter of photovoltaic modules *Prog. Photovolt.: Res. Appl.* **22** 1159-71
- [10] Kempe M D, Miller D C and Wohlgemuth J H et al. 2015 Field testing of thermoplastic encapsulants in high-temperature installations *Energy Sci. Eng.* **3** 565-80
- [11] Zhu J, Koehl M and Hoffmann S et al. 2016 Changes of solar cell parameters during damp-heat exposure *Prog. Photovolt.: Res. Appl.* **24** 1346-58
- [12] Schneller E J, Brooker R P and Shiradkar N S et al. 2016 Manufacturing metrology for c-Si module reliability and durability Part III: Module manufacturing *Renew. Sustain. Energy. Rev.* **59** 992-1016
- [13] Chiang S Y, Chou T L, Shih Z H, Hong H F and Chiang K N 2011 Life prediction of HCPV under thermal cycling test condition *Microelectron. Eng.* **88** 785-90
- [14] Hoffmann S and Koehl M 2014 Effect of humidity and temperature on the potential-induced degradation *Prog. Photovolt.: Res. Appl.* **22** 173-79